COMPUTATIONAL CONTINUUM MECHANICS
ВЫЧИСЛИТЕЛЬНАЯ МЕХАНИКА СПЛОШНЫХ СРЕД
Computational Continuum Mechanics. 2021. Vol. 14. No. 3. pp. 349-356
DOI: 10.7242/1999-6691/2021.14.3.29

CONVECTION IN VISCOPLASTIC FLUIDS IN RECTANGULAR CAVITIES AT LATERAL HEATING

T.P. Lyubimova[1], M.G. Kazimardanov[1] and A.V. Perminov[2]

[1]*Institute of Continuous Media Mechanics UB RAS, Perm, Russian Federation*
[2]*Perm National Research Polytechnic University, Perm, Russian Federation*

The paper is devoted to the study of convective motions of viscoplastic fluids in closed two-dimensional rectangular domains with different aspect ratios under lateral heating. The problem was solved numerically using the ANSYS Fluent software. The Herschel-Bulkley model was chosen for describing the rheological behavior of the fluid. Under certain rheological parameters, this model was transformed into a Newtonian fluid model, whose behavior was also simulated as a limiting case. Based on the calculated results, the dependences of the maximum value of the stream function in the cavity on the Rayleigh number are plotted. It was found that at small Rayleigh numbers the intensity of motion is close to zero. At a certain threshold value of the Rayleigh number there is a sharp increase in the intensity of motion, and a further increase in the Rayleigh number causes an almost linear growth of the maximum value of the stream function. For each of the considered ratios of cavity sides, the "threshold" values of the Rayleigh number, at which a sharp increase in the intensity of motion of liquid is observed, were determined. The obtained values of Rayleigh numbers turned out to be close to the "threshold" values of the Rayleigh number for the Bingham fluid found in the works of other authors earlier. The fields of the stream function and the square root of the second invariant of the viscous stress tensor were obtained for different values of the Rayleigh number and different aspect ratios. The scenarios of rearrangement of quasisolid motion zones with increasing Rayleigh number were compared with the available results for the Bingham fluid.

Key words*:* convection, non-Newtonian fluid, Herschel-Bulkley model, viscoplastic fluid, unyielded zone, numerical simulation

1. Introduction

The motion of viscoplastic fluids due to convection in vertical rectangular cavities with different aspect ratios under lateral heating conditions is studied. Non-Newtonian fluids are widely used in the chemical, oil refining, automotive and aviation industries. Among others motor oils used in car engines and aircraft engine gearboxes have the properties of non-Newtonian fluids, and are able, due to the formation of a thin layer on the walls of the unit, to reduce friction between the parts. The study of the flows of non-Newtonian fluid is of great engineering and scientific interest.

The convective flow of viscoplastic fluids in closed cavities was first considered in [1-3]. In [1], the problem of convection in a viscoplastic fluid in a cavity with a square cross section under lateral heating is solved within the framework of the regularized Williamson's rheological model, which allows calculations in a unified way in the entire cavity. It is found that, in contrast to the case of a Newtonian fluid, at small values of the Rayleigh number, only a weak convective motion is observed, and when the Rayleigh number reaches a certain value, there is a sharp increase in the intensity of the motion. The structure of unyielded zones has been determined for different values of the Rayleigh number. The nature of the intensity of motion in the cavity and the evolution of unyielded zones depending on the Rayleigh number is discovered. In [3], two variational principles were formulated, and by means of numerical minimization of the corresponding functional for the Rayleigh number, the top and bottom approximations, denoting the range of occurrence of convective motion of Schwedow-Bingham fluid in rectangular cavities at varying aspect ratios, were obtained. Later, the same problem was solved in [4] for other aspect ratios of the cavity. Here, the threshold values of parameters at which convective motion occurs in the fluid were also calculated, and turned out to be in good agreement with the results published earlier in [2]. Two-dimensional steady-state modes of thermal convection in a viscoplastic fluid in rectangular cavities with different aspect ratios under side heating within the two-viscosity model proposed in [5] were studied in [6, 7]. The dependences of the Nusselt number on the Bingham number were obtained for different cavity sizes.

Email addresses for correspondence: lyubimovat@mail.ru

© The Author(s), 2021. Published by Institute of Continuous Media Mechanics.
This is an Open Access article, distributed under the terms of the Creative Commons Attribution-NonCommercial 4.0 (CC BY-NC 4.0), which permits unrestricted re-use, distribution, and reproduction in any medium, provided the original work is properly cited.

2. Statement of the task

Consider a two-dimensional planar problem of convection in a viscoplastic fluid moving in vertical rectangular cavities with ratio of sides $A = L/H = 1/1;\ 1/2;\ 1/4$ when heated from the side in the field of gravity (Fig. 1). To describe free thermal convection in liquid we will use equations of motion in Boussinesq:

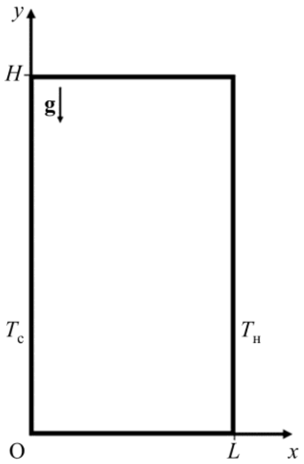

Fig. 1. Geometry of the calculation domain.

$$\rho\frac{\partial u}{\partial t} + \rho u\frac{\partial u}{\partial x} + \rho v\frac{\partial u}{\partial y} = -\frac{\partial p}{\partial x} + \left(\frac{\partial \tau_{xx}}{\partial x} + \frac{\partial \tau_{xy}}{\partial y}\right),$$

$$\rho\frac{\partial v}{\partial t} + \rho u\frac{\partial v}{\partial x} + \rho v\frac{\partial v}{\partial y} = -\frac{\partial p}{\partial y} + \left(\frac{\partial \tau_{xy}}{\partial x} + \frac{\partial \tau_{yy}}{\partial y}\right) + \rho g\beta\left(T - T_c\right),$$

$$\frac{\partial u}{\partial x} + \frac{\partial v}{\partial y} = 0,$$

$$\rho C_p\frac{\partial T}{\partial t} + \rho u C_p\frac{\partial T}{\partial x} + \rho v C_p\frac{\partial T}{\partial y} = \kappa\left(\frac{\partial T^2}{\partial x^2} + \frac{\partial T^2}{\partial y^2}\right).$$

Here: u — x velocity component; v — y velocity component; ρ — density; p — pressure; $\mathbf{g}$ — gravitational acceleration; β — coefficient of thermal expansion; C_p — specific heat capacity; T — temperature; T_c — cold wall temperature; κ — thermal conductivity coefficient; τ_{xx}, τ_{xy}, τ_{yy} — components of the viscous stress tensor.

The Herschel-Balkley equation [8] is used to describe the rheological properties of a fluid:

$$\boldsymbol{\tau} = \mu_0\boldsymbol{\gamma} \qquad \text{при} \quad \gamma < \gamma_0,$$

$$\boldsymbol{\tau} = \left(\frac{\tau_0}{\gamma} + K\cdot\boldsymbol{\gamma}^{n-1}\right)\boldsymbol{\gamma} \qquad \text{при} \quad \gamma > \gamma_0,$$

$$\gamma_0 = \frac{\tau_0}{\mu_0}, \qquad \gamma = \left[\frac{1}{2}\boldsymbol{\gamma}:\boldsymbol{\gamma}\right]^{1/2},$$

where $\boldsymbol{\tau}$ — viscous stress tensor, $\boldsymbol{\gamma}$ — strain rate tensor, τ_0 — yield stress, γ_0 — yield shear rate, μ_0 — yield viscosity, K — consistency coefficient, n — nonlinearity index. At low shear rates ($\gamma < \gamma_0$) the viscosity of the fluid μ_0 is very high. The rheological curve corresponding to the Herschel-Balkley equation for $n = 1$, is shown in Figure 2. In the case of the Herschel-Balkley rheological model, it turns into a rheological curve for a viscoplastic fluid in the limit ($\gamma_0 \to 0$).

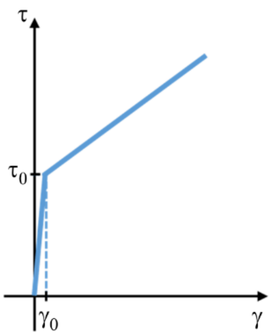

Fig. 2. Herschel-Balkley fluid rheological curve for $n=1$.

We consider all boundaries of the cavity to be solid and assume that the sticking conditions are satisfied on them. At the vertical boundaries of the cavity, we set different constant temperature $T_н$ and T_c, and at the horizontal boundaries we consider the temperature varying linearly:

$$x = 0: \quad u = 0, \quad T = T_c \quad ,$$

$$x = L: \quad u = 0, \quad T = T_н, \quad T_н > T_c,$$

$$y = 0: \quad v = 0, \quad T = \frac{T_н - T_c}{L}x + T_c,$$

$$y = H: \quad v = 0, \quad T = \frac{T_н - T_c}{L}x + T_c.$$

3. Numerical research method

The calculations were performed using the ANSYS Fluent application software package. To solve a system of equations in Fluent, the First Order Upwind discretization scheme was chosen. A fixed time step of 0.1 s was assumed. Such a time step was chosen based on the fulfillment of the scheme stability condition and the minimum time required for test calculations. The computational meshes were constructed using the ICEM CFD mesh generator. The square cells forming it had a linear size of 0.1 mm. The meshes consisting of 100×100, 100×200 and 100×400 cells were tested. The spatial step size was determined on the basis of preliminary calculations on different meshes and analysis of the convergence of the solution when the mesh step was reduced in size.

The value τ_0 is taken from [1]. In order to establish the value of the consistency coefficient, preliminary calculations with different K in the range 0,01–0,1 kg·s^{n-2}/m were carried out. Such value K was chosen that allows one to most accurately describe the threshold nature of occurrence of convection in Schwedow-Bingham liquid when heated from the side.

In all calculations fixed material parameters of liquid and constant value of gravitational acceleration were set: $\rho = 998$ kg/m^3; $\beta = 0{,}0015$ K^{-1}; $C_p = 4183$ J/kg·K; $\kappa = 0{,}599$ W/m·K; $\mu_0 = 10$ kg/m·s; $\tau_0 = 0{,}000285$ N/m^2; $n = 1{,}0$; K = 0,01 kg·s^{n-2}/m; $g = 9{,}81$ m/s^2. The basic calculations are performed at $\gamma_0 = 2{,}85 \cdot 10^{-5}$ 1/s. Verification calculations carried out at $\gamma_0 = 7{,}13 \cdot 10^{-6}$ 1/s, gave very close results (the patterns of unyielded zones coincided in the scale of the graph), which made it possible to consider the Herschel-Balkley model with $\gamma_0 = 2{,}85 \cdot 10^{-5}$ 1/s to be valid: it simulates convection in a viscoplastic fluid quite accurately.

It should be noted that in the calculations in the ANSYS Fluent package, the parameters have a dimensional form. It is the dimensional fields of the stream function Ψ and the components of the viscous stress tensor, as well as the maximum value of the stream function $\Psi_{\max}$ in the cavity depending on the dimensionless parameter - the Rayleigh number, $\mathrm{Ra} = \dfrac{g \beta \Delta T L^3}{\nu \chi}$ ($\Delta T = T_{\text{н}} - T_{\text{c}}$, ν — kinetic viscosity, χ — thermal conductivity, L — geometric dimension of the cavity), that are given below (the dimensionality of the stream function in kg/s is due to the fact that in Fluent it is represented as its ratio to the liquid density).

The found fields of the components of the viscous stress tensor were used to determine the unyielded zones. As in [1], the criterion for selecting unyielded zones was the condition $\sqrt{T_2} < \tau_0$, $T_2 = (1/2)\tau_{ij}\tau_{ij}$, where T_2 — second invariant of the viscous stress tensor.

4. Calculation results

Calculations for the chosen values of the aspect ratio A were performed at Rayleigh numbers in the range $\mathrm{Ra} = 0...16000$. It showed that for all A and Ra in the cavity there is one-vortex convective motion directed counterclockwise (see Fig. 3 at a fixed value of Rayleigh number).

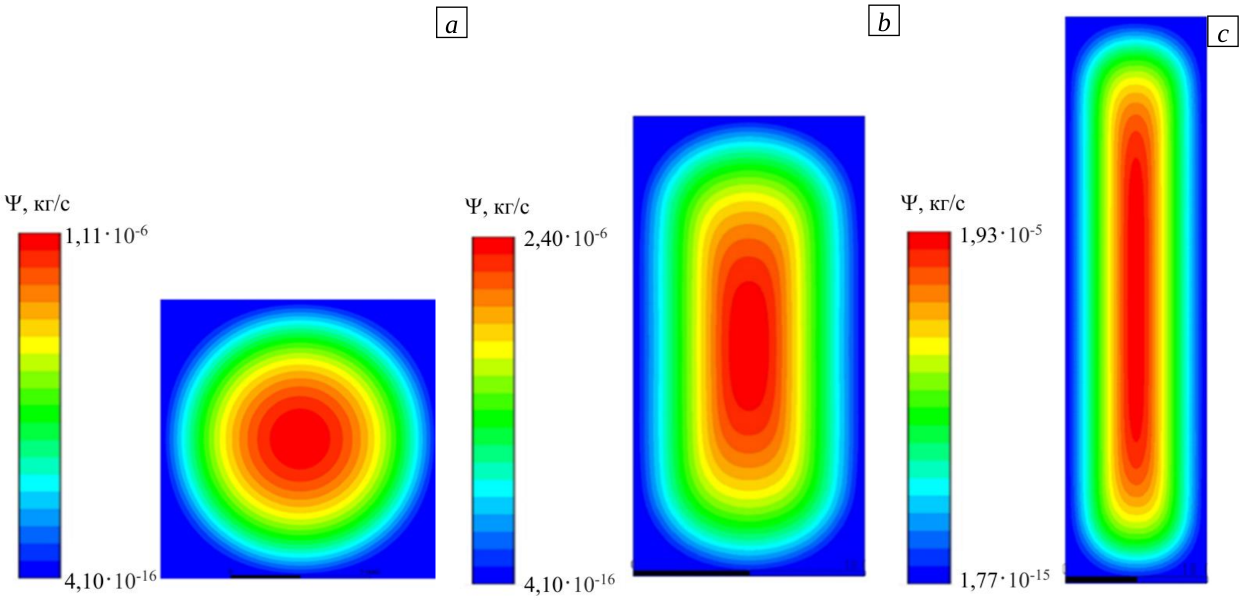

Fig. 3. Fields of the stream function at the value of Rayleigh number $\mathrm{Ra} = 5000$ and different values of the ratio of the cavity sides A: 1/1 (*a*); 1/2 (*b*); 1/4 (*c*) .

Figure 4 shows the dependences of the maximum values of the stream function $\Psi_{\max}$ on the number Ra also for different values of the geometric parameter A. As can be seen, in all three cases for small values of the Rayleigh number the intensity of motion is close to zero; the values of $\gamma < \gamma_0$. In the limiting case of a viscoplastic fluid this means a complete absence of motion. After some threshold value of Rayleigh number with its further growth there is a sharp increase of intensity of motion, which leads to practically linear growth of $\Psi_{\max}$. Similar behavior was noted in [1, 2]. The threshold values of the Rayleigh number, when passing through which there is a sharp increase in the intensity of motion, are: 6750 for $A = 1/1$, 4900 for $A = 1/2$ and 4050 for $A = 1/4$. When determining the threshold value Ra for each of the ratios, the criterion was the appearance of a narrow closed zone of shear flow.

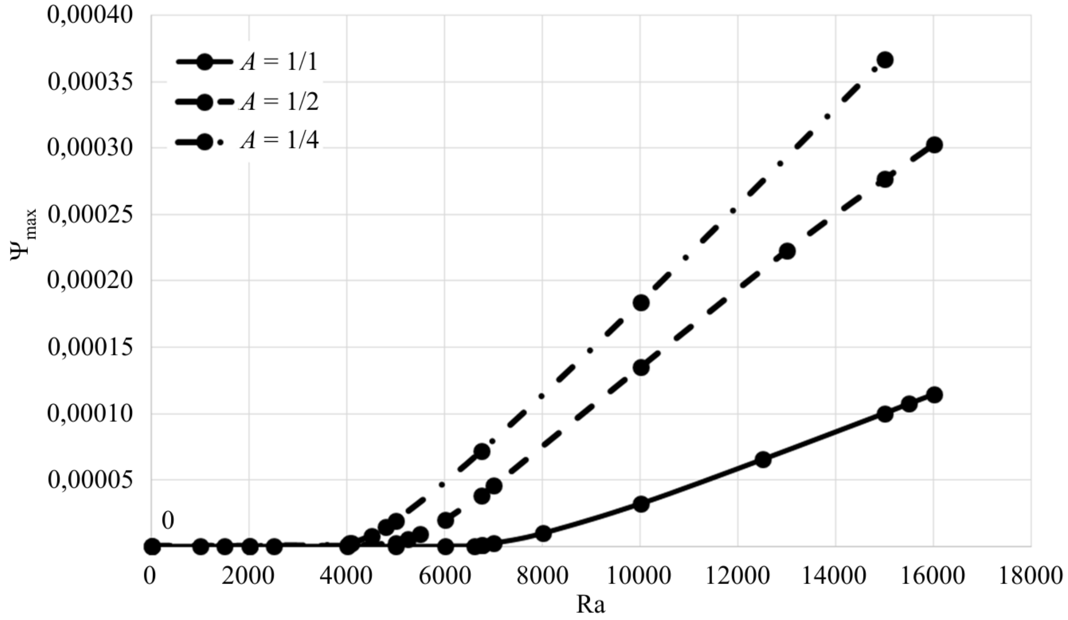

Fig. 4. Dependence of the maximum value of the stream function on the Rayleigh number.

For the case of a square cavity, the variational principle was formulated in [1], and on its basis the analytical expression linking the Rayleigh threshold number with the dimensionless yield strength of the Schwedow-Bingham fluid was obtained. For the parameter values chosen in the present work, this formula gives a threshold value equal to $\mathrm{Ra} \approx 6355$, and the threshold value found numerically and corresponding to the Herschel-Balkley fluid was $\mathrm{Ra} \approx 6750$, which is close to the value given above for the Schwedow-Bingham fluid.

In [3], two variational principles are formulated and, by means of numerical minimization of corresponding functional for values of Rayleigh number, approximations from above and below are obtained, denoting the range of occurrence of Schwedow-Bingham fluid motion in rectangular cavities with aspect ratio $A = 1/1; 1/2; 1/5$ during side heating. As a result, the Rayleigh number varies: for a square cavity from 5950 to 7740, for a rectangular region with $A = 1/2$ from 4860 to 5750. The Rayleigh threshold numbers calculated in this paper for the Herschel-Bulkley fluid are as follows: 6750 — for a square cavity; 4900 — for a rectangular cavity with $A = 1/2$. Both values are in the interval given in [3].

Figure 5 shows the structure of unyielded zones at different Rayleigh numbers for the case of a square cavity. The unyielded zones were considered to be the regions with $\sqrt{T_2}$ less than the fluidity limit τ_0. Inside such zones the shear velocities tend to zero and the fluid actually moves as a solid [1]. The unyielded zones in this and the following figures are shaded in white. As can be seen, at $\mathrm{Ra} = 6500$ the value $\sqrt{T_2}$ exceeds the yield strength only in very narrow zones near the midpoints of the cavity boundaries (Fig. 5a). At $\mathrm{Ra} \approx 6750$ a narrow closed zone of shear flow emerges adjacent to the cavity boundaries (Fig. 5b). A further increase in the Rayleigh number leads to a decrease in the area of unyielded zones and a change in their shape. At $\mathrm{Ra} \approx 15000$ the unyielded zone in the center of the cavity, as in [1] for the Williamson fluid, takes the shape of a cross (Fig. 5c). The shape of the unyielded zone remains unchanged during steady-state (stationary) motion, which also agrees with [1]. At $\mathrm{Ra} \approx 16000$, when the unyielded zone in the center of the cavity disappears, and stagnant unyielded areas remain in its corners.

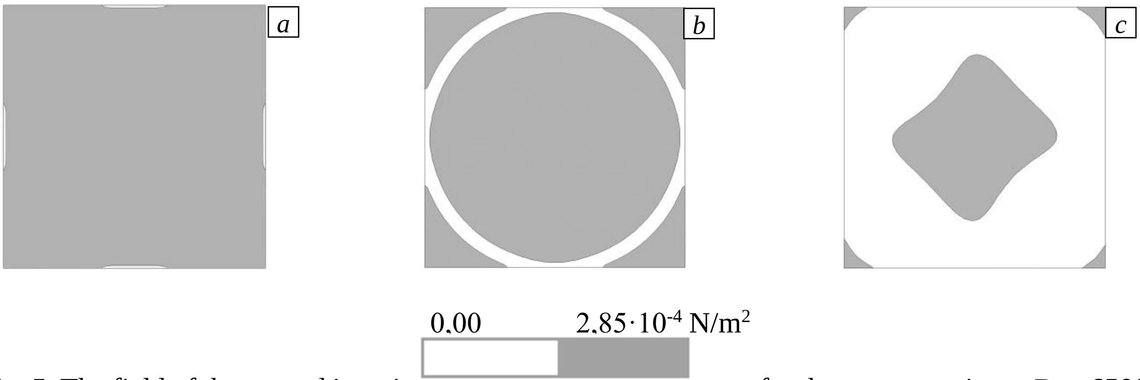

Fig. 5. The field of the second invariant of the viscous stress tensor for the square cavity at Ra : 6500 (*a*), 6750 (*b*), 15000 (*c*) .

Figure 6 shows the evolution of the unyielded and shear motion zones of a viscoplastic fluid with increasing Rayleigh number for a rectangular cavity with parameter $A = 1/2$. As can be seen, at $\mathrm{Ra} = 4800$ (Fig. 6a) the parameter $\sqrt{T_2}$ exceeds the yield strength only in narrow zones near the middle of the cavity boundaries, similar to what happens in a square cavity (see Fig. 5a).

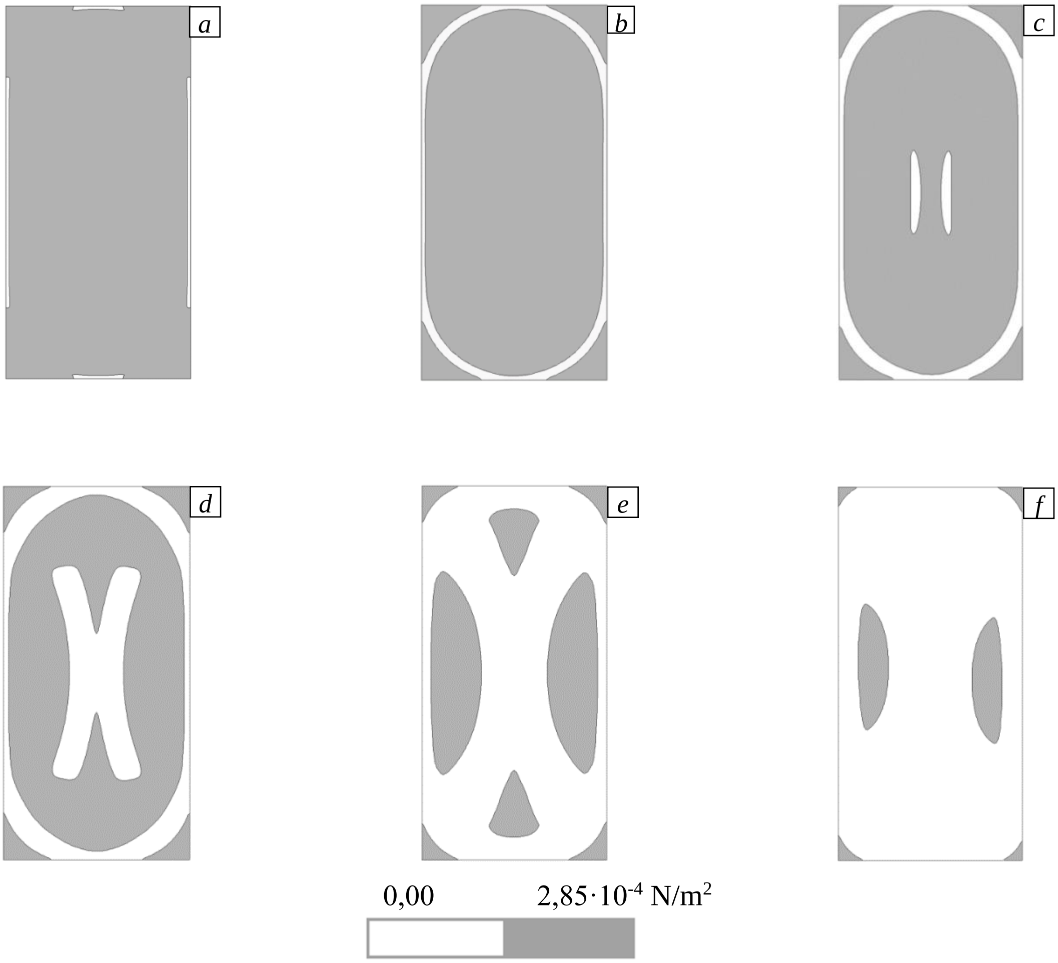

Fig. 6. Field of the second invariant of the viscous stress tensor for a rectangular cavity with $A = 1/2$ at Ra 4800 (*a*), 4900 (*b*), 5000 (*c*), 5250 (*d*), 6000 (*e*), 10000 (*f*).

At $\mathrm{Ra} \approx 4900$ (Fig. 6b), a narrow closed zone of shear flow emerges adjacent to the cavity boundaries, where $\sqrt{T_2} > \tau_0$, and the central part is still occupied by a unyielded zone in which $\sqrt{T_2} < \tau_0$. In the corners, unyielded stagnant zones are observed, which do not disappear completely even at large numbers of Ra.

As the Rayleigh number increases, two separate small liquid zones appear in the center of the unyielded zone (Fig. 6c), which increase as the Rayleigh number increases. These liquid zones join and form one X-shaped zone (Fig. 6d), which merges with the annular zone of shear flow in the range of values of the Rayleigh number 5250…6000. Thus, the unyielded zone in the center of the cavity splits into 4 isolated parts (Fig. 6e). At $\mathrm{Ra} \approx 10^4$ The unyielded zones near the upper and lower boundaries of the cavity disappear, and the remaining zones decrease in size (Fig. 6f)). At $\mathrm{Ra} \approx 2 \cdot 10^4$ only unyielded areas in the corners of the cavity are observed.

Figure 7 shows the evolution of unyielded zones with increasing Rayleigh number for a rectangular cavity with $A = 1/4$. Results of calculations have shown that at $\mathrm{Ra} < 4050$ (Рис. 7*a*, for $\mathrm{Ra} = 4000$), similar to the case with $A = 1/2$ (see Fig. 6a), narrow liquid zones arise near the middle of the cavity boundaries, where $\sqrt{T_2} > \tau_0$, but in contrast to the case of $A = 1/2$, simultaneously with the confined liquid zones, a narrow vertical strip of the liquid zone appears in the center of the cavity.

When $\mathrm{Ra} \geq 4050$ (Fig. 7b), there is a narrow closed zone of shear flow near the cavity boundaries, adjacent to the cavity boundaries, the liquid zone in the center of the cavity becomes larger in this case. As the Rayleigh number increases, an X-shaped liquid zone (Fig. 7c) is formed in the central part of the cavity, as in the case with $A = 1/2$ (Fig. 6d), which merges with the closed zone of shear flow near the cavity boundaries as the Rayleigh number further increases, similarly to the case with $A = 1/2$. Four isolated unyielded zones are formed in the center of the cavity (Fig. 7d).

The structure of the unyielded zones, shown in Figures 6b and 7d is close to the threshold structure of these zones for the Schwedow-Bingham fluid, first obtained using variational methods in [3], and later confirmed numerically [4-6].

At $\mathrm{Ra} \approx 6750$, the upper and lower boundaries of the cavity of unyielded zones disappear, similar to what happens in a rectangular cavity with $A = 1/2$. At $\mathrm{Ra} \approx 2 \cdot 10^4$ the vertical boundaries of the cavity, unyielded zones cease to exist and only stagnant zones remain in the corners of the cavity. Thus, as the vertical size of the cavity increases, the evolution of the unyielded and shear motion zones of the viscoplastic fluid with increasing Rayleigh number value is close to the situation that takes place in the case of a flat vertical layer [9].

The patterns of unyielded zones obtained for various aspect ratios at Rayleigh numbers slightly exceeding the threshold values (see. Fig. 5b, $\mathrm{Ra} \approx 6750$; 6b, $\mathrm{Ra} \approx 10000$; 7b), are close to the patterns corresponding to the threshold patterns of unyielded zones in the Schwedow-Bingham fluid, established using variational methods for the square cavity in [1], and for the rectangular cavity in [3], and confirmed later for the Schwedow-Bingham fluid in [4]. However, in the narrow intervals between the values of Ra, at which zones first appear in the cavity where $\sqrt{T_2} > \tau_0$ (see. Рис. 5*a*, $\mathrm{Ra} \approx 6500$; 6*a*, $\mathrm{Ra} \approx 4800$; 7*a*, $\mathrm{Ra} \approx 4000$), and the values of Ra, corresponding to Figures 5b, 6b, 7b, the patterns of unyielded zones differ from those obtained earlier for the Schwedow-Bingham liquid.

5. Conclusion

The convective flow of a viscoplastic fluid in a vertical rectangular cavity under lateral heating for three different aspect ratios has been studied within the part of the Herschel-Bulkley model. The fields of the stream function, the second invariant of the viscous stress tensor, and the dependences of the maximum value of the stream function in the cavity on the Rayleigh number were obtained for different values of the Rayleigh number.

The threshold values of Rayleigh numbers, at which a sharp growth of the intensity of motion is observed, are determined. For a square cavity, the threshold Rayleigh number was equal to $\mathrm{Ra} \approx 6750$, for a cavity with geometric parameter - $A = 1/2$ — $\mathrm{Ra} \approx 4900$, for $A = 1/4$ — $\mathrm{Ra} \approx 4050$. These values agree well with the results obtained earlier by other authors. As the vertical size of the cavity increases, the threshold value of Rayleigh number decreases and approaches the threshold value corresponding to the Schwedow-Bingham limit case $A \to 0$ (see [9]).

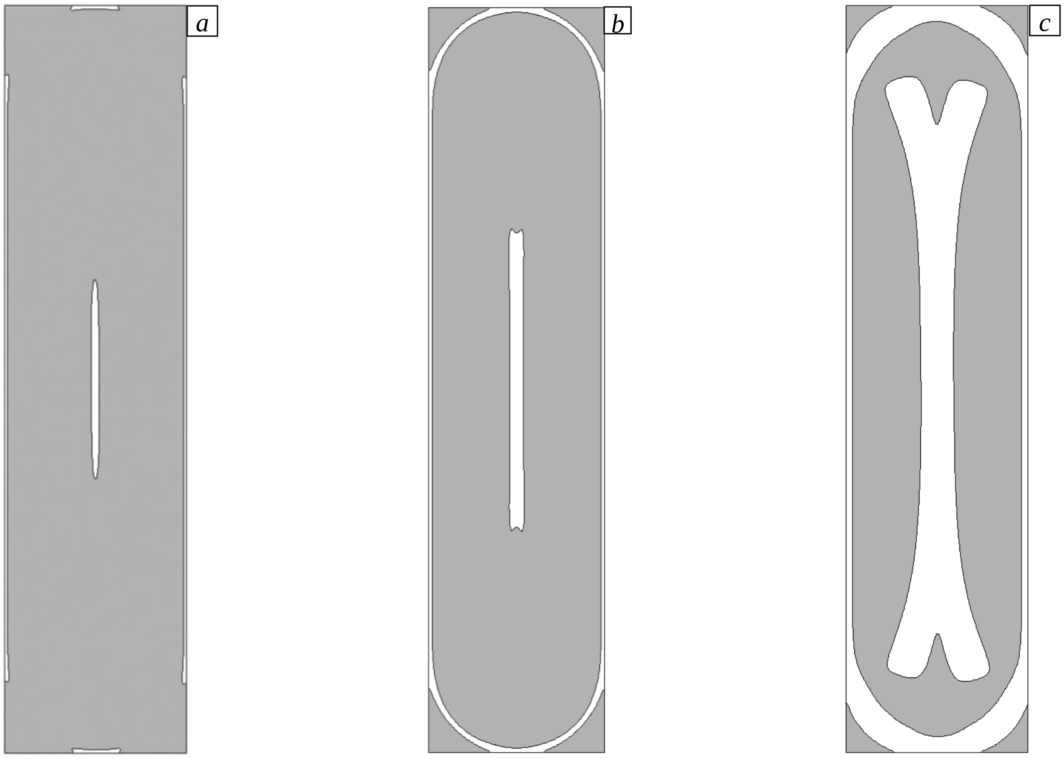

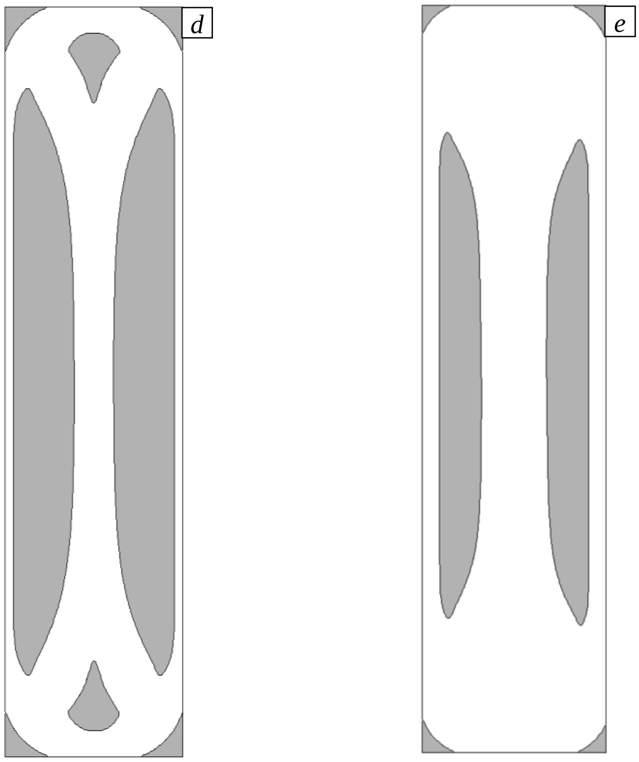

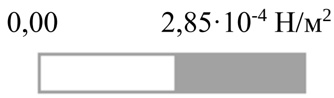

Fig. 7. The field of the second invariant of the viscous stress tensor for a rectangular cavity with $A = 1/4$ at Ra 4000 (a), 4050 (b), 4500 (c), 4800 (f), 6750 (e).

Numerical simulations have shown that the structures of unyielded zones in the Herschel-Balkley fluid at Rayleigh numbers insignificantly exceeding the threshold values are close to the structures established earlier for the viscoplastic Schwedow-Bingham fluid [1, 3, 4]. However, in narrow intervals where, on the one hand, the Rayleigh number values at which liquid zones first appear in the cavity and, on the other hand, the Rayleigh numbers corresponding to the appearance of a developed convective flow in a viscoplastic fluid differ from the structures for the Schwedow-Bingham fluid in unyielded zones. This is due to the fact that the behavior of the Schwedow-Bingham and Herschel-Balkley fluids is qualitatively different at stresses below the yield stress point: in the Schwedow-Bingham fluid there is no motion at all, while in the Herschel-Balkley fluid there is a weak convective motion.

References

1. Lyubimova T.P. Numerical investigation of convection in a viscoplastic liquid in a closed region. *Fluid Dyn.*, 1977, vol. 12, pp. 1-5. https://doi.org/10.1007/BF01074616
2. Lyubimova T.P. Convective motions of a viscoplastic fluid in a rectangular region. *Fluid Dyn.*, 1979, vol. 14, pp. 747-750. https://doi.org/10.1007/BF01409817
3. Lyubimov D.V., Lyubimova T.P. O primenenii variatsionnykh printsipov v zadache o konvektsii vyazkoplastichnoy zhidkosti [*On application of variational principles to the problem of thermal convection of viscoplastic fluid*] // Konvektivnyye techeniya [Convective Flows], 1979, no. 1, pp. 81-86.
4. Vikhansky A. On the onset of natural convection of Bingham liquid in rectangular enclosures. *J. Non-Newtonian Fluid Mech.*, 2010, vol. 165, pp. 1713-1716. https://doi.org/10.1016/j.jnnfm.2010.09.003
5. O'Donovan E.J., Tanner R.I. Numerical study of the Bingham squeeze film problem. *J. Non-Newtonian Fluid Mech.*, 1984, vol. 15, pp. 75-83. https://doi.org/10.1016/0377-0257(84)80029-4
6. Turan O., Poole R.J., Chakraborty N. Aspect ratio effects in laminar natural convection of Bingham fluids in rectangular enclosures with differentially heated side walls. *J. Non-Newtonian Fluid Mech.*, 2011, vol. 166, pp. 208-230. https://doi.org/10.1016/j.jnnfm.2010.12.002
7. Turan O., Chakraborty N., Poole R.J. Laminar Rayleigh-Bénard convection of yield stress fluids in a square enclosure. *J. Non-Newtonian Fluid Mech.*, 2012, vol. 171-172, pp. 83-96. https://doi.org/10.1016/j.jnnfm.2012.01.006
8. Herschel W.H., Bulkley R. Konsistenzmessungen von Gummi-Benzollosungen [Consistency measurements of gum benzene solutions]. *Kolloid-Zeitschrift*, 1926, vol. 39, pp. 291-300. https://doi.org/10.1007/BF01432034
9. Yang W.-J., Yeh H.-C. Free convective flow of Bingham plastic between two vertical plates. *J. Heat Transfer.*, 1965, vol. 87, pp. 319-320. https://doi.org/10.1115/1.3689104

The authors declare no conflict of interests.
The paper was received on 08.04.2021.
The paper was accepted for publication on 06.07.2021.